Supplementary Materials

Appendix 1. Available data on substance use and general psychopathology in participants. Substance use data is a count of the number of participants that endorse consuming alcohol, tobacco or cannabis with a certain frequency. The CIS-R score is given as median (interquartile range).

Supplementary Table 1. Similarity between ALSPAC cohort and sample recruited for the MRI study in terms of gender, childhood IQ, and general psychopathology. IQ and CIS-R scores are reported as median (interquartile range)

	Psychotic Experiences			Healthy Controls		
	Not In MRI	In MRI		Not In MRI	In MRI	
Total Sample	n = 306	n = 126		n = 4153	n = 126	
Female	191 (62.4%)	87 (69.1%)		2306 (55.5%)	77 (61.1%)	
	n = 221	n = 104		n = 3473	n = 114	
IQ at age 8	105 (24)	106.5 (19)	χ^2 = 0.74, p = 0.39	107 (23)	111 (22)	χ^2 = 7.46, p = 0.001
	n = 275	n = 115		n = 3831	n = 121	
CIS-R	9 (11)	10 (15)	χ^2 = 4.38, p = 0.04	3 (6)	4 (10)	χ^2 = 8.43, p = 0.004

CIS-R = revised Clinical Interview Schedule, carried out at age 18.

Supplementary Table 2. Comparison of self-reported substance use at age 18 in the ALSPAC cohort and the sample recruited for the MRI study. The MRI sample is then broken down into our current labelling of PEs to gauge if the groups differ in their substance use or if there is any indication of abuse.

	Psychotic Experiences		Healthy Controls		MRI Study Sample		
	Not In MRI	In MRI	Not In MRI	In MRI	Healthy Controls	Transient PEs	Persistent PEs
Alcohol Consumption							
Never	27	10	508	22	16	10	3
Not anymore	13	2	96	5	5	0	2
Once or twice	24	17	384	13	12	13	5
Monthly	100	48	1719	51	45	26	26
Weekly	53	23	628	15	14	11	13
Daily	2	0	15	0	0	0	0
Tobacco Consumption							
Never	36	14	516	19	16	9	7
Not anymore	21	14	193	8	8	4	10
Once or twice	30	9	596	21	18	7	4
Monthly	12	5	227	4	4	2	3
Weekly	12	8	120	2	2	2	6
Daily	30	10	176	5	4	6	5
Cannabis Consumption							
Never	99	60	2115	82	73	38	27
Once or twice	17	10	134	4	11	6	5
Not anymore	22	10	416	12	4	1	9
Monthly	18	5	194	8	7	5	1
Weekly	10	3	58	2	1	1	3
Daily	7	1	16	0	0	0	1

Appendix 2. MRI processing details

Cortical morphometry was assessed using Freesurfer version 5.3 (surfer.nmr.mgh.harvard.edu). The image processing pipeline is fully automated and has been described in greater detail[1–4]. In short, Freesurfer aims to extract the cortical grey matter by identifying the boundaries with white matter as well as the dura and/or cerebrospinal fluid and warp the cortical grey matter to a stereotactic space. Cortical thickness (CT) can be computed as the distance between the pial surface and white matter boundary. The local gyrification index (lGI) is computed as the ratio of the amount of grey matter visible on a sulcal-filled outline of the surface and the corresponding amount on the pial surface. The lGI and CT maps were smoothed using a Gaussian filter; full width at half maximum of 5mm and 10mm, respectively. Freesurfer QA tools were used to inspect the quality of image processing and summary quality assessment measures are reported in supplementary table 1.

To correct for multiple comparisons, a cluster-wise correction was performed using a precomputed Monte Carlo simulation[5] of a z-distribution with a vertex-wise threshold of $p<0.001$ and a cluster-wise threshold of $p<0.05$. A Bonferroni correction was applied to adjust for both cerebral hemispheres.

Data were analysed in ExploreDTI v4.8.3[6] (http://exploredti.com) and processing steps have been described in greater detail in Drakesmith et al[7–9]. Images were corrected for head motion, distortions induced by eddy currents, and field inhomogeneities[10,11]. In the presence of head rotation, the B-matrix was reoriented as described by Leemans and Jones[11]. Field inhomogeneities were corrected through non-linear registration to a synthetic T_1-weighted volume computed from a mcDESPOT processing pipeline (see Drakesmith et al[8] for full details and quality control). Deterministic tractography was carried out using a dampened Lucy-Richardson algorithm[12] to estimate the peak in fibre orientation distribution function (fODF) across a 3x3x3mm grid (stepsize=1mm, fODF threshold=0.05, angular threshold=45°, streamline lengths=30 – 300mm).

Alterations in cortical morphometry were implemented as volumes of interest (VOI) for atlas-based tractography. First, clusters identified at group level were transformed to each participant's native space to produce a VOI. This volume was then dilated and eroded to fill any holes inside and trimmed using cortical ribbon masks to restrict the VOI to the cortical grey matter. A boundary-based cost function was used to produce a transformation matrix from diffusion space to Freesurfer native space and the inverse was applied to transform VOIs to diffusion space. Diffusion metrics were extracted from streamlines passing or ending in the VOI.

Supplementary Table 3. Freesurfer summary data quality measures from the initial T_1-weighted volumes and statistical output of group comparisons

		Healthy Controls	Transient PEs	Persistent PEs	
n		111	67	69	
Euler Number[a]	Left Hemisphere	-158.0 (41.5)	-158.0 (44.3)	-168.4 (68.1)	$F_{(2,244)} = 1.03$, $p = 0.35$
	Right Hemisphere	-161.9 (42.4)	-153.4 (38.9)	-168.8 (66.3)	$F_{(2,244)} = 1.65$, $p = 0.20$
CNR[b]	Grey/White	1.22 (0.07)	1.21 (0.08)	1.21 (0.09)	$F_{(2,244)} = 0.95$, $p = 0.39$
	Grey / CSF	1.23 (0.06)	1.22 (0.07)	1.23 (0.08)	$F_{(2,244)} = 0.72$, $p = 0.49$

CNR = Contrast-to-Noise Ratio, CSF = Cerebrospinal Fluid

[a] The Euler Number is calculated as $2-2g$ where g is the number of defects. The closer this number is to 2, the better the quality of the data for cortical surface reconstruction. Throughout the Freesurfer pipeline, all defects were corrected and the final reconstructed surface had a Euler Number of 2.

[b] The CNR represents the ratio between the difference in signal intensity between regions of different tissue types and the background noise.

Appendix 3. Supplementary Results

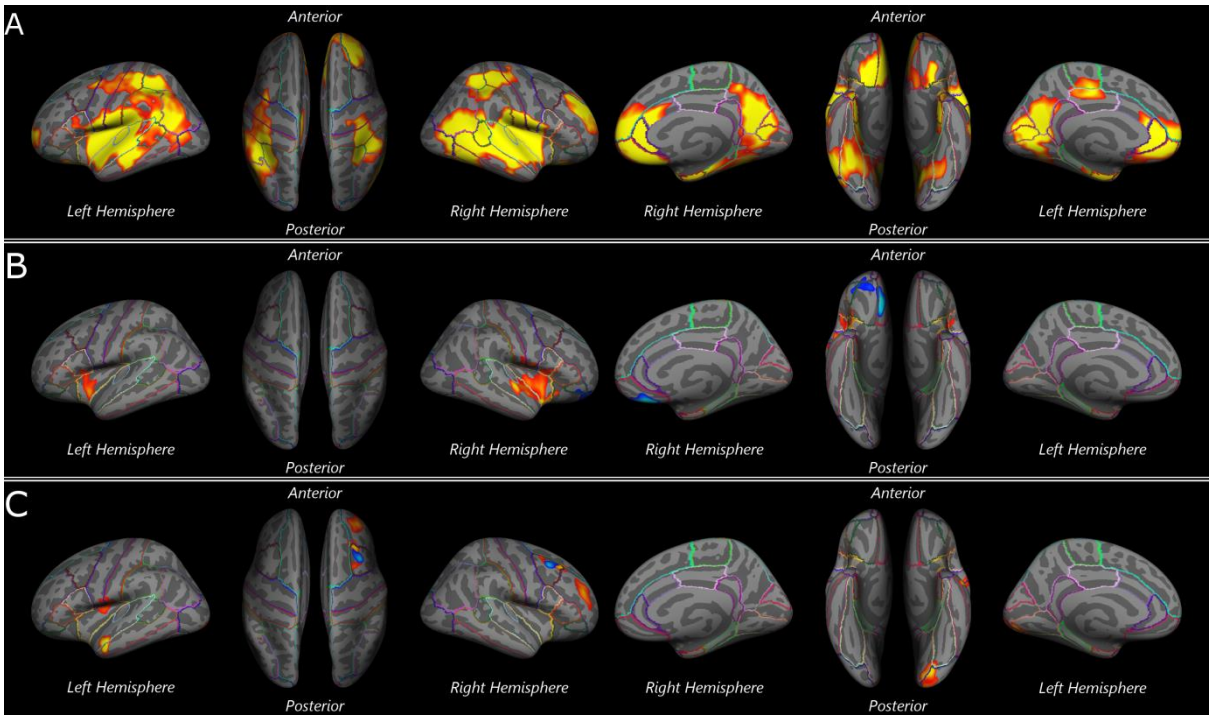

Supplementary Figure 1. Main Effects of total brain volume (TBV) and IQ on cortical morphometry in the whole sample (n=247) and the effects associated with PEs in the PRS subsample (n=180). Clusters are overlaid on the MNI305 template that shows the outline of Desikan-Killiany atlas parcellations[13]. Row A: Regions showing a positive association between the local gyrification index (lGI) and TBV (red-yellow). Row B: Regions shown to be associated with childhood IQ scores, positive associations were found for lGI (red-yellow), but negative associations with cortical thickness (CT) were also seen (blue-light blue). Row C: Significant effects of PEs in the PRS subsample that highlight reductions in lGI in persistent PEs (red-yellow) and an increase in CT in transient PEs (blue-light blue).

Supplementary Table 4. Summary of clusters where gyrification (lGI) or cortical thickness (CT) showed positive associations with total brain volume (TBV) or childhood IQ.

Metric	**Effect**	**Cluster Peak**	**Cluster Size (mm^2)**	**MNI Coordinates**			**p**	**z**
				X	Y	Z		
CT	IQ	R mOFG	489.5	7.2	30.7	-23.6	0.0036	2.06
		R lOFG	460.3	18	43.9	-15.5	0.0056	1.96
lGI	IQ	R Ins	2118.1	39.9	-2.5	-18.5	0.0002	2.63
		R PrCG	369.2	50.4	-1.9	7.1	0.0333	1.51
		L Ins	512.6	-36.0	-2.3	-7.4	0.0056	1.96
CT	TBV	R STG	413.1	48.5	-12.8	-8.0	0.0092	1.84
lGI	TBV	R PCG	21179.5	55.7	-12.1	16.5	0.0002	2.63
		R rACG	7733.7	7.6	37.2	4.5	0.0002	2.63
		R PCG	3795.8	40.3	-33.7	60.3	0.0002	2.63
		L rACG	4430.2	-6.7	34.7	-0.1	0.0002	2.63
		L Ins	20327.0	-35.8	-16.2	5.0	0.0002	2.63
		L PC	4929.2	-16.5	-58.1	18.8	0.0002	2.63
		L PCG	844.3	-9.1	-20.5	38.3	0.0002	2.63

mOFG = medial Orbitofrontal Gyrus, lOFG = lateral Orbitofrontal Gyrus, Ins = Insular Cortex, PrCG = Precentral Gyrus, STG = Superior Temporal Gyrus, PCG = Postcentral Gyrus, rACG = rostral Anterior Cingulate Gyrus, PC = Precuneus

Supplementary Table 5. Differences in cortical morphometry in the PRS subsample (n=180) in relation to group membership and interaction effects with TBV, IQ, and PRS. Region and coordinates are based on the location of the cluster peak.

Metric	Effect	Region	Cluster Size (mm^2)	MNI Coordinates			p value	z score
				X	Y	Z		
lGI	Group[c]	L MTG	568.5	-55.1	-0.5	-27.5	0.0022	2.17
lGI	Group × TBV[c]	L MTG	437.7	-54.7	0.4	-28.5	0.0149	1.72
lGI	Group × TBV[c]	R rMFG	834.0	29.8	40.3	20.0	0.0002	2.63
lGI	Group × TBV[c]	R cMFG	467.0	30.0	23.5	43.9	0.0108	1.95
lGI	Group × TBV[c]	L LOG	1319.3	-22.4	-85.1	-10.0	0.0002	2.63
lGI	Group × TBV[c]	L PrCG	660.7	-54.9	-5.4	8.9	0.0006	2.43
CT	Group × TBV[c]	R cMFG	310.4	37.3	15.9	50.5	0.0365	1.48
lGI	Group × PRS[d]	L PCG	1911.4	-21.5	-39.4	57.0	0.0002	2.63
lGI	Group × PRS[d]	L IPG	617.9	-40.6	-80.4	16.6	0.0018	2.21
lGI	Group × PRS[d]	R MTG	433.4	51.7	6.5	-32.9	0.0144	1.73

MTG=Middle Temporal Gyrus, rMFG = rostral Middle Frontal Gyrus, cMFG = caudal Middle Frontal Gyrus, LOC = Lateral Occipital Cortex, PrCG = Precentral Gyrus, PCG = Postcentral Gyrus, IPL = Inferior Parietal Gyrus

[a] Cluster-wise corrected p-value based on a precomputed Monte Carlo simulation with a z-distribution with a vertex-wise threshold of $p < 0.001$ and a cluster threshold of $p < 0.05$.

[b] Computed based on the cluster-wise p-value

[c] Effect was found for the linear contrast (HC > Transient PEs > Persistent PEs)

[d] Effect was found for the quadratic contrast (HC < Transient PEs > Persistent PEs)

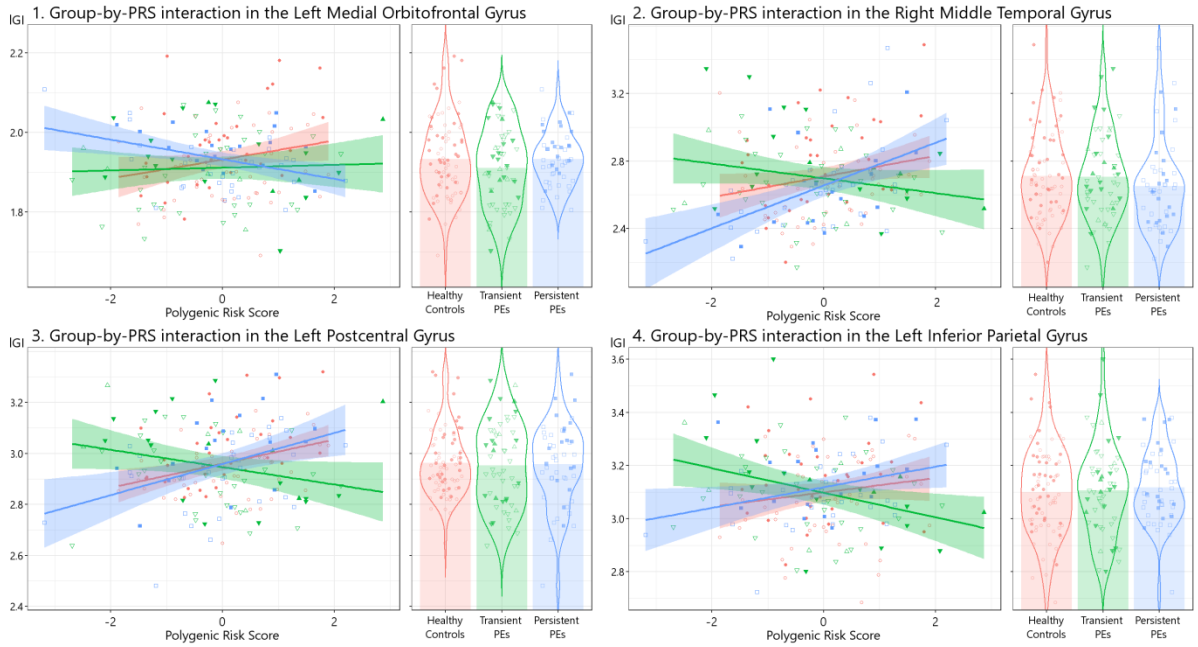

Supplementary Figure 2. Plots of group-by-PRS interaction effects that demonstrate the different slopes for gyrification (lGI) as a function of the standardised score for polygenic risk for schizophrenia (PRS). Healthy controls are shown as red circles, transient PEs as green triangles, and persistent PEs as blue squares. Males are denoted as filled symbols and females using open symbols. A linear contrast (HC > Transient PEs > Persistent PEs) was fitted to the regressors for the PRS in each group to test an interaction effect (see panel 1, also reported in the main body of text). A quadratic contrast (HC < Transient PEs > Persistent PEs) was then subsequently tested to examine the assumption that transient PEs lie intermediate. This was found to not be the case in several clusters that highlighted a different slope for transient PEs relative to HC and persistent PEs (see panels 2-4). Emergent and resilient PEs are denoted as an upward-facing and downward-facing triangles, respectively.

Supplementary Table 6. Average size of the volumes of interest for each group in native space.

Sample	Region	Healthy Controls	Transient PEs	Persistent PEs	Test Statistic
n=242	L MTG	545.78 (84.99)	520.70 (84.19)	530.05 (91.96)	$\chi^2_{(2)} = 4.28$, p = 0.12
n=242	L LOG	932.16 (144.94)	891.82 (148.24)	923.46 (141.42)	$\chi^2_{(2)} = 3.72$, p = 0.16
n=242	L LG	276.75 (56.88)	263.02 (56.39)	256.83 (54.40)	$\chi^2_{(2)} = 6.98$, p = 0.03
n=242	R cMFG	2052.63 (308.19)	2015.36 (364.37)	1990.82 (314.34)	$\chi^2_{(2)} = 1.73$, p = 0.42
n=178	L mOFG	571.62 (92.47)	558.96 (124.11)	542.08 (90.32)	$\chi^2_{(2)} = 3.09$, p = 0.21
n=178	L PrCG	1217.77 (170.54)	1179.54 (160.27)	1199.44 (166.81)	$\chi^2_{(2)} = 2.03$, p = 0.36
n=178	L IPG	546.48 (135.39)	521.79 (108.54)	499.85 (111.93)	$\chi^2_{(2)} = 3.39$, p = 0.18
n=178	R MTG	455.15 (77.81)	447.85 (70.29)	429.94 (71.43)	$\chi^2_{(2)} = 4.58$, p = 0.10

MTG=Middle Temporal Gyrus, LOC = Lateral Occipital Cortex, LG = Lingual Gyrus, cMFG = caudal Middle Frontal Gyrus, mOFG = medial Orbitofrontal Gyrus, PrCG = Precentral Gyrus, IPG = Inferior Parietal Gyrus

Supplementary Table 7. Output from Hartigan's Dip Test; assessing the presence of a non-unimodal distribution of tract length for each VOI.

n=242	L MTG	L LOC	L LG	R cMFG
Hartigan's Dip Test	D = 0.02, p = 0.97	D = 0.02, p = 0.65	D = 0.02, p = 0.99	D = 0.02, p = 0.90
n = 178	L mOFG	L PrCG	L IPG	R MTG
Hartigan's Dip Test	D = 0.02, p = 0.87	D = 0.02, p = 0.91	D = 0.03, p = 0.56	D = 0.02, p = 0.98

MTG=Middle Temporal Gyrus, LOC = Lateral Occipital Cortex, LG = Lingual Gyrus, cMFG = caudal Middle Frontal Gyrus, mOFG = medial Orbitofrontal Gyrus, PrCG = Precentral Gyrus, IPG = Inferior Parietal Gyrus

Supplementary Table 8. Summary of the diffusion metrics in each group for each volume of interest identified in the main analysis (n=247) of the cortical surface. The mean and standard deviation are reported for each measure and an adjusted confidence interval is given for the bootstrapped estimate of the difference between HC and each group.

Region			Healthy Controls	Transient PEs	Persistent PEs
			n = 110	n = 66	n = 66
L MTG	FA ($x10^{-1}$)	Mean (SD)	3.44 (0.34)	3.37 (0.31)	3.40 (0.32)
		Difference (95% CI)		-0.03 – 0.16	-0.06 – 0.14
	MD ($x10^{-4}$ mm^2/s^{-1})	Mean (SD)	8.71 (0.38)	8.63 (0.36)	8.71 (0.41)
		Difference (95% CI)		-0.04 – 0.19	-0.13 – 0.11
	AD ($x10^{-4}$ mm^2/s^{-1})	Mean (SD)	12.01 (0.55)	11.83 (0.53)	11.97 (0.67)
		Difference (95% CI)		**0.006 – 0.33[a]**	-0.15 – 0.22
	RD ($x10^{-4}$ mm^2/s^{-1})	Mean (SD)	7.06 (0.43)	7.03 (0.39)	7.09 (0.39)
		Difference (95% CI)		-0.09 – 0.15	-0.14 – 0.11
	Length (mm)	Mean (SD)	82.62 (17.15)	80.52 (13.80)	82.41 (13.44)
		Difference		-2.55 – 6.73	-4.19 – 4.85

		(95% CI)			
	Streamlines	Mean (SD)	605.02 (159.08)	561.42 (138.15)	600.62 (188.88)
		Difference (95% CI)		-0.47 – 88.67	-5.15 – 57.06
	Volume (cm^3)	Mean (SD)	22.53 (6.7)	20.45 (5.35)	21.84 (7.51)
		Difference (95% CI)		**0.28 -3.86[a]**	-1.54 – 2.83
L LOC	FA ($x10^{-1}$)	Mean (SD)	3.66 (0.45)	3.65 (0.44)	3.73 (0.39)
		Difference (95% CI)		-0.13 – 0.14	-0.20 – 0.05
	MD ($x10^{-4}$ mm^2/s^{-1})	Mean (SD)	9.11 (0.53)	9.21 (0.76)	9.23 (0.63)
		Difference (95% CI)		-0.33 – 0.09	-0.29 – 0.07
	AD ($x10^{-4}$ mm^2/s^{-1})	Mean (SD)	12.95 (0.89)	13.06 (1.07)	13.19 (0.98)
		Difference (95% CI)		-0.42 – 0.18	-0.54 – 0.03
	RD ($x10^{-4}$ mm^2/s^{-1})	Mean (SD)	7.20 (0.53)	7.28 (0.74)	7.24 (0.58)
		Difference (95% CI)		-0.31 – 0.11	-0.22 – 0.12
	Length	Mean (SD)	107.53 (16.94)	107.24 (15.83)	110.82 (16.74)
		Difference		-4.48 – 5.43	-8.16 – 2.00

		(95% CI)			
	Streamlines	Mean (SD)	1152.87 (414.22)	1064.64 (300.86)	1144.58 (331.20)
		Difference (95% CI)		-11.77 – 202.52	-92.15 – 129.36
	Volume (mm^3)	Mean (SD)	43.13 (12.19)	40.19 (10.05)	42.07 (11.09)
		Difference (95% CI)		-0.14 – 6.50	-2.12 – 4.84
L LG	FA ($x10^{-1}$)	Mean (SD)	3.12 (0.44)	3.12 (0.41)	3.01 (0.44)
		Difference (95% CI)		-0.19 – 0.17	-0.02 – 0.29
	MD ($x10^{-4}$ mm^2/s^{-1})	Mean (SD)	9.43 (0.59)	9.47 (0.6)	9.65 (0.74)
		Difference (95% CI)		-0.33 – 0.27	-0.41 – 0.11
	AD ($x10^{-4}$ mm^2/s^{-1})	Mean (SD)	12.71 (0.83)	12.78 (0.93)	12.85 (1.04)
		Difference (95% CI)		-0.30 – 0.21	-0.53 – 0.33
	RD ($x10^{-4}$ mm^2/s^{-1})	Mean (SD)	7.80 (0.62)	7.82 (0.68)	8.05 (0.72)
		Difference (95% CI)		-0.28 – 0.25	-0.55 – 0.01
	Length	Mean (SD)	86.47 (15.91)	87.01 (15.32)	84.99 (15.22)
		Difference		-6.25 – 6.16	-6.81 – 5.63

		(95% CI)			
	Streamlines	Mean (SD)	543.51 (176.97)	495.14 (142.20)	536.97 (173.31)
		Difference (95% CI)		-25.00 – 82.00	-25.00 – 78.00
	Volume (mm^3)	Mean (SD)	23.11 (6.24)	21.38 (5.80)	22.53 (6.41)
		Difference (95% CI)		-2.15 – 4.07	-2.27 – 3.89
R cMFG	FA ($x10^{-1}$)	Mean (SD)	3.20 (0.28)	3.23 (0.28)	3.23 (0.26)
		Difference (95% CI)		-0.08 – 0.10	-0.05 – 0.12
	MD ($x10^{-4}$ mm^2/s^{-1})	Mean (SD)	9.36 (0.49)	9.33 (0.56)	9.43 (0.55)
		Difference (95% CI)		-0.11 – 0.25	-0.27 – 0.12
	AD ($x10^{-4}$ mm^2/s^{-1})	Mean (SD)	12.53 (0.57)	12.55 (0.57)	12.67 (0.66)
		Difference (95% CI)		-0.26 – 0.24	-0.36 – 0.13
	RD ($x10^{-4}$ mm^2/s^{-1})	Mean (SD)	7.78 (0.53)	7.73 (0.62)	7.81 (0.56)
		Difference (95% CI)		-0.17 – 0.26	-0.19 – 0.19
	Length	Mean (SD)	62.42 (8.70)	64.16 (8.81)	62.32 (8.29)
		Difference		-5.18 – 0.68	-4.84 – 1.89

		(95% CI)			
	Streamlines	Mean (SD)	1858.58 (442.88)	1860.49 (446.53)	1844.76 (572.53)
		Difference (95% CI)		-107.42 – 199.00	-68.00 – 184.00
	Volume (mm^3)	Mean (SD)	49.74 (11.48)	51.08 (12.42)	49.31 (14.78)
		Difference (95% CI)		-3.77 – 4.51	-2.12 – 4.82

MTG=Middle Temporal Gyrus, LOC = Lateral Occipital Cortex, LG = Lingual Gyrus, cMFG = caudal Middle Frontal Gyrus

[a] Confidence interval range does not indicate the presence of an effect after Bonferroni correction for multiple comparisons ($1 - \frac{\alpha}{m}$) where *m* is equal to four (FA, MD, AD, RD) or three (Length, Volume, Number of Streamlines)

Supplementary Table 9. Summary of the diffusion metrics in the smaller sample (n=180) for each cluster that had been identified. The mean and standard deviation are reported for each measure and an adjusted confidence interval is given for the bootstrapped estimate of the difference between HC and each group.

Region			Healthy Controls	Transient PEs	Persistent PEs
			n=78	n=52	n=48
L mOFG	FA ($x10^{-1}$)	Mean (SD)	2.78 (0.29)	2.76 (0.27)	2.99 (0.35)
		Difference (95% CI)		-0.09 – 0.15	**-0.34 – -0.08[a]**
	MD ($x10^{-4}$ mm^2/s^{-1})	Mean (SD)	9.47 (0.57)	9.58 (0.66)	9.41 (0.41)
		Difference (95% CI)		-0.34 – 0.11	-0.21 – 0.26
	AD ($x10^{-4}$ mm^2/s^{-1})	Mean (SD)	12.23 (0.65)	12.34 (0.76)	12.40 (0.57)
		Difference (95% CI)		-0.28 – 0.14	**-0.05 – -0.07[a]**
	RD ($x10^{-4}$ mm^2/s^{-1})	Mean (SD)	8.09 (0.60)	8.20 (0.66)	7.91 (0.48)
		Difference (95% CI)		-0.39 – 0.08	-0.19 – 0.38
	Length (mm)	Mean (SD)	69.92 (10.12)	68.49 (9.10)	73.11 (10.12)
		Difference (95% CI)		-29.74 – 5.92	-5.81 – 3.49

	Streamlines	Mean (SD)	920.64 (199.62)	831.94 (239.92)	945.52 (488.60)
		Difference (95% CI)		**24.00 – 168.00[a]**	-86.00 – 99.00
	Volume (cm^3)	Mean (SD)	31.74 (7.51)	28.71 (7.63)	33.44 (16.47)
		Difference (95% CI)		-1.43 – 4.00	-3.47 – 0.97
L PCG	FA ($x10^{-1}$)	Mean (SD)	3.82 (0.22)	3.85 (0.24)	3.85 (0.22)
		Difference (95% CI)		-0.09 – 0.11	-0.08 – 0.12
	MD ($x10^{-4}$ mm^2/s^{-1})	Mean (SD)	9.21 (0.42)	9.21 (0.52)	9.23 (0.54)
		Difference (95% CI)		-0.26 – 0.16	-0.41 – 0.17
	AD ($x10^{-4}$ mm^2/s^{-1})	Mean (SD)	13.03 (0.45)	13.09 (0.49)	13.09 (0.49)
		Difference (95% CI)		-0.38 – 0.04	-0.35 – 0.12
	RD ($x10^{-4}$ mm^2/s^{-1})	Mean (SD)	7.30 (0.46)	7.27 (0.57)	7.30 (0.59)
		Difference (95% CI)		-0.24 – 0.24	-0.39- 0.21
	Length	Mean (SD)	103.28 (6.45)	103.68 (7.41)	104.40 (7.21)
		Difference (95% CI)		-2.95 – 4.54	-3.79 – 1.12

	Streamlines	Mean (SD)	2431.68 (495.32)	2327.27 (390.24)	2413.17 (278.53)
		Difference (95% CI)		-218.60 – 267.00	-236.00 – 86.00
	Volume (mm^3)	Mean (SD)	67.10 (11.84)	64.62 (11.26)	67.02 (8.35)
		Difference (95% CI)		-4.77 – 5.61	-5.78 – 2.58
L IPG	FA ($x10^{-1}$)	Mean (SD)	2.89 (0.36)	2.93 (0.35)	2.94 (0.34)
		Difference (95% CI)		-0.26 – 0.07	-0.29 – 0.02
	MD ($x10^{-4}$ mm^2/s^{-1})	Mean (SD)	8.07 (0.22)	8.10 (0.31)	8.13 (0.26)
		Difference (95% CI)		-0.15 – 0.09	**-0.19 – -0.02[a]**
	AD ($x10^{-4}$ mm^2/s^{-1})	Mean (SD)	10.60 (0.45)	10.67 (0.43)	10.71 (0.39)
		Difference (95% CI)		-0.33 – 0.09	-0.38 – 0.08
	RD ($x10^{-4}$ mm^2/s^{-1})	Mean (SD)	6.80 (0.27)	6.81 (0.38)	6.84 (0.32)
		Difference (95% CI)		-0.10 – 0.12	-0.16 – 0.13
	Length	Mean (SD)	55.73 (13.26)	55.28 (11.26)	57.97 (14.19)
		Difference (95% CI)		-9.10 – 3.58	-10.3 – 3.03

	Streamlines	Mean (SD)	425.54 (147.18)	408.14 (135.31)	399.60 (136.36)
		Difference (95% CI)		-63.00 – 64.00	-24.00 – 84.00
	Volume (mm^3)	Mean (SD)	14.19 (5.67)	13.66 (4.93)	13.84 (5.65)
		Difference (95% CI)		-2.34 – 1.79	-1.97 – 2.41
R MTG	FA ($x10^{-1}$)	Mean (SD)	3.33 (0.31)	3.36 (0.31)	3.32 (0.31)
		Difference (95% CI)		-0.16 – 0.16	-0.09 – 0.17
	MD ($x10^{-4}$ mm^2/s^{-1})	Mean (SD)	9.02 (0.62)	9.14 (0.73)	9.25 (0.85)
		Difference (95% CI)		-0.56 – 0.14	-0.44 – 0.14
	AD ($x10^{-4}$ mm^2/s^{-1})	Mean (SD)	12.31 (0.80)	12.50 (0.89)	12.59 (1.05)
		Difference (95% CI)		-0.38 – 0.28	-0.50 – 0.33
	RD ($x10^{-4}$ mm^2/s^{-1})	Mean (SD)	7.38 (0.60)	7.47 (0.71)	7.59 (0.80)
		Difference (95% CI)		-0.48 – 0.15	**-0.52 – -0.004**[a]
	Length	Mean (SD)	82.02 (18.08)	83.27 (17.33)	84.88 (20.35)
		Difference (95% CI)		-7.25 – 9.94	-9.67 – 5.16

	Streamlines	Mean (SD)	470.92 (164.41)	445.62 (145.26)	466.90 (166.32)
		Difference (95% CI)		-66.00 - 80.00	-83.00 – 62.00
	Volume (mm^3)	Mean (SD)	20.32 (7.94)	19.48 (6.97)	21.09 (8.70)
		Difference (95% CI)		-2.85 – 4.19	-4.98 – 2.23

mOFG = medial Orbitofrontal Gyrus, PrCG = Precentral Gyrus, IPG = Inferior Parietal Gyrus

[a] Confidence interval range does not indicate the presence of an effect after Bonferroni correction for multiple comparisons ($1 - \frac{\alpha}{m}$) where *m* is equal to four (FA, MD, AD, RD) or three (Length, Volume, Number of Streamlines)

Supplementary Table 10. Adjusted confidence intervals around bootstrapped estimates of the correlation coefficient between the local gyrification index (lGI) and metrics of underlying white matter.

Region		Pearson's Correlation Coefficient (95% CI)
	Measure	lGI
L MTG	FA	-0.26 – 0.04
	MD	**0.06 – 0.34***
	AD	-0.06 - 0.22
	RD	**0.09 – 0.36***
	Streamlines	**0.06 – 0.33***
	Length	**-0.28 – -0.02[a]**
	Volume	-0.06 – 0.20
L LOC	FA	**-0.25 – -0.03***
	MD	**-0.30 – -0.06***
	AD	**-0.35 – -0.12***
	RD	-0.22 – 0.03
	Streamlines	-0.24 – 0.02
	Length	**-0.29 – -0.08***
	Volume	**-0.26 – -0.03***
L LG	FA	-0.01 – 0.24
	MD	-0.16 – 0.09
	AD	-0.08 – 0.17
	RD	-0.21 – 0.05
	Streamlines	**0.27 – 0.49***
	Length	-0.11 – 0.13
	Volume	**0.29 – 0.50***

R cMFG	FA	-0.22 – 0.01
	MD	-0.13 – 0.12
	AD	-0.19 – 0.05
	RD	-0.10 – 0.16
	Streamlines	**0.11 – 0.44***
	Length	**-0.30 – -0.08***
	Volume	**0.05 – 0.32***

MTG=Middle Temporal Gyrus, LOC = Lateral Occipital Cortex, LG = Lingual Gyrus, cMFG = caudal Middle Frontal Gyrus

[a] Confidence intervals did cross through zero following Bonferroni correction ($1 - \frac{\alpha}{m}$) where *m* is equal to four (FA, MD, AD, RD) or three (Streamlines, Length, Volume).

* Estimated effect survived Bonferroni correction

Supplementary Table 11. Estimates for the correlation between white matter indices and the polygenic risk score (PRS) as well as the average local gyrification index (lGI) obtained from identified clusters. Confidence intervals (CI) were obtained by acquiring bootstrapped estimates of the correlation coefficient between white matter metrics and the lGI or PRS.

		Pearson's Correlation Coefficient (95% CI)	
Region	Measure	lGI	PRS
L mOFG	FA	-0.20 – 0.11	-0.13 – 0.16
	MD	-0.09 – 0.19	-0.15 – 0.12
	AD	-0.12 – 0.15	-0.15 – 0.12
	RD	-0.08 – 0.20	-0.15 – 0.13
	Streamlines	**0.12 – 0.32***	-0.10 – 0.19
	Length	-0.19 – 0.09	-0.18 – 0.10
	Volume	**0.09 – 0.30***	-0.09 – 0.20
L PCG	FA	-0.06 – 0.21	-0.19 – 0.07
	MD	-0.25 – 0.03	-0.06 – 0.23
	AD	-0.19 – 0.09	-0.09 – 0.21
	RD	-0.28 – 0.002	-0.07 – 0.22
	Streamlines	**0.08 – 0.33***	-0.17 – 0.13
	Length	-0.19 – 0.06	-0.10 – 0.15
	Volume	**0.01 – 0.29a**	-0.11 – 0.16
L IPG	FA	-0.20 – 0.09	-0.03 – 0.25
	MD	-0.08 – 0.21	-0.13 – 0.18
	AD	-0.13 – 0.14	-0.01 – 0.25
	RD	-0.08 – 0.22	-0.02 – 0.10

	Streamlines	**0.16 – 0.41***	-0.01 – 0.26
	Length	-0.14 – 0.15	-0.03 – 0.24
	Volume	**0.04 – 0.31***	**0.02 – 0.27[a]**
R MTG	FA	-0.01 – 0.29	-0.10 – 0.20
	MD	-0.18 – 0.13	-0.12 – 0.14
	AD	-0.13 – 0.19	-0.12 – 0.16
	RD	-0.21 – 0.10	-0.13 – 0.12
	Streamlines	**0.06 – 0.34***	-0.12 – 0.16
	Length	-0.06 – 0.24	-0.08 – 0.19
	Volume	**0.003 – 0.31[a]**	-0.12 – 0.17

mOFG = medial Orbitofrontal Gyrus, PrCG = Precentral Gyrus, IPG = Inferior Parietal Gyrus

[a] Confidence intervals did cross through zero following Bonferroni correction ($1 - \frac{\alpha}{m}$) where *m* is equal to four (FA, MD, AD, RD) or three (Streamlines, Length, Volume).

* Estimated effect survived Bonferroni correction

Supplementary References

1. Dale AM, Fischl B, Sereno MI. Cortical Surface-Based Analysis: I. Segmentation and Surface Reconstruction. *Neuroimage*. 1999;9(2):179-194. doi:10.1006/nimg.1998.0395.

2. Fischl B, Sereno MI, Dale AM. Cortical Surface-Based Analysis II: Inflation, Flattening, and a Surface-Based Coordinate System. *Neuroimage*. 1999;9(2):195-207. doi:10.1006/nimg.1998.0396.

3. Fischl B. FreeSurfer. *Neuroimage*. 2012;62(2):774-781. doi:10.1016/j.neuroimage.2012.01.021.

4. Schaer M, Cuadra MB, Schmansky N, Fischl B, Thiran J-P, Eliez S. How to Measure Cortical Folding from MR Images: a Step-by-Step Tutorial to Compute Local Gyrification Index. *J Vis Exp*. 2012;(59):e3417-e3417. doi:10.3791/3417.

5. Hagler DJ, Saygin AP, Sereno MI. Smoothing and cluster thresholding for cortical surface-based group analysis of fMRI data. *Neuroimage*. 2006;33(4):1093-1103. doi:10.1016/j.neuroimage.2006.07.036.

6. Leemans A, Jeurissen B, Sijbers J, Jones D. ExploreDTI: a graphical toolbox for processing, analyzing, and visualizing diffusion MR data. In: *Proceedings 17th Scientific Meeting, International Society for Magnetic Resonance in Medicine*. Vol 17. ; 2009:3537.

7. Drakesmith M, Caeyenberghs K, Dutt A, et al. Schizophrenia-like topological changes in the structural connectome of individuals with subclinical psychotic experiences. *Hum Brain Mapp*. 2015;36(7):2629-2643. doi:10.1002/hbm.22796.

8. Drakesmith M, Dutt A, Fonville L, et al. Mediation of Developmental Risk Factors for Psychosis by White Matter Microstructure in Young Adults With Psychotic Experiences. *JAMA Psychiatry*. 2016;73(4):396-406. doi:10.1001/jamapsychiatry.2015.3375.

9. Drakesmith M, Dutt A, Fonville L, et al. Volumetric, relaxometric and diffusometric correlates of psychotic experiences in a non-clinical sample of young adults. *NeuroImage Clin*. 2016;12:550-558. doi:10.1016/j.nicl.2016.09.002.

10. Wu M, Chang LC, Walker L, et al. Comparison of EPI distortion correction methods in diffusion tensor MRI using a novel framework. *Med Image Comput Comput Interv*. 2008;11(Pt 2):321-329. doi:10.1016/j.bbamem.2015.02.010.Cationic.

11. Leemans A, Jones DK. The B-matrix must be rotated when correcting for subject motion in DTI data. *Magn Reson Med*. 2009;61(6):1336-1349. doi:10.1002/mrm.21890.

12. Dell'Acqua F, Scifo P, Rizzo G, et al. A modified damped Richardson-Lucy algorithm to reduce isotropic background effects in spherical deconvolution. *Neuroimage*. 2010;49(2):1446-1458. doi:10.1016/j.neuroimage.2009.09.033.

13. Desikan RS, Ségonne F, Fischl B, et al. An automated labeling system for subdividing the human cerebral cortex on MRI scans into gyral based regions of interest. *Neuroimage*. 2006;31(3):968-980. doi:10.1016/j.neuroimage.2006.01.021.